Supporting information for: "EPR spectroscopy of iron- and nickel-doped [ZnAl]-layered double hydroxides: modeling active sites in heterogeneous water oxidation catalysts"

Richard I. Sayler[†], Bryan M. Hunter[†], Wen Fu[†], Harry B. Gray[‡], and R. David Britt*[†]

[†]Department of Chemistry, University of California at Davis, Davis, California 95616, United States
[‡]Division of Chemistry and Chemical Engineering, California Institute of Technology, Pasadena, California 91125, United States

Table of Contents

I) Induction Coupled Plasma - Mass Spectrometry

The ICP-MS samples were prepared by dissolving 2.1 mg of “1%” Fe:[ZnAl]-LDH in 5.3 mL of 3% nitric acid (trace metal basis), 4.2 mg of the “5%” Fe:[ZnAl]-LDH in 10.5 mL of 3% nitric acid (trace metal basis) and 2.5 mg of “1%” Ni:[ZnAl]-LDH in 6.3 mL 3% nitric acid (trace metal basis). Each of these samples was further diluted 100-fold in 3% nitric acid before ICP-MS (**Table S1**).

Sample	% Fe added	% Ni added	% Zn added	% Al added	% Fe final	% Ni final	% Zn final	% Al final
1%-[Fe:ZnAl]-LDH	1	0	75	24	1	0.1	79	20
5%-[Fe:ZnAl]-LDH	5	0	75	20	4.5	0.05	77.5	18
1%-[Ni:ZnAl]-LDH	0	1	74	25	0.2	2	66	30

Table S1. Molar percent of metal ions added during synthesis *versus* final molar percent of metal ions in prepared materials, as determined by ICP-MS.

II) Powder X-ray Diffraction

The material phase was confirmed using powder X-ray diffraction (XRD). There was good agreement with the literature pattern for [ZnAl]-LDH. Slight variations were seen when comparing the [ZnAl]-LDH diffraction peaks with [Fe:ZnAl]-LDH, owing to slight changes in the unit cell due to the addition of Fe(III) (Figure S2). Powder X-ray diffraction (XRD) data were collected at room temperature using a Bruker D8 ADVANCE Eco at 40kV and 25mA. The data were collected in the 5°-70° 2θ range with a step size of 0.0143° and a dwell time of 0.5 s/step. The intensities were normalized.

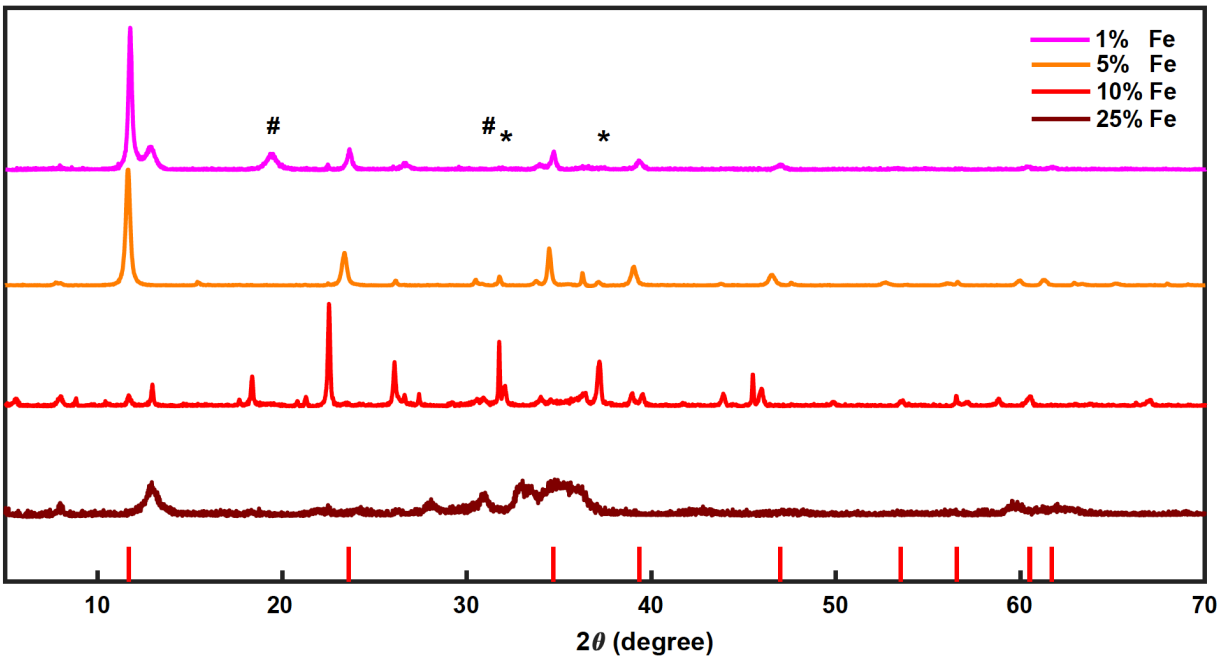

Figure S1. Powder XRD patterns of Fe-doped [ZnAl]-LDH with different concentrations of iron. Red lines: ZnAl layered double hydroxide (COD 9015034), #: Al_2O_3 (COD1101168), *: ZnO (COD 2300113)

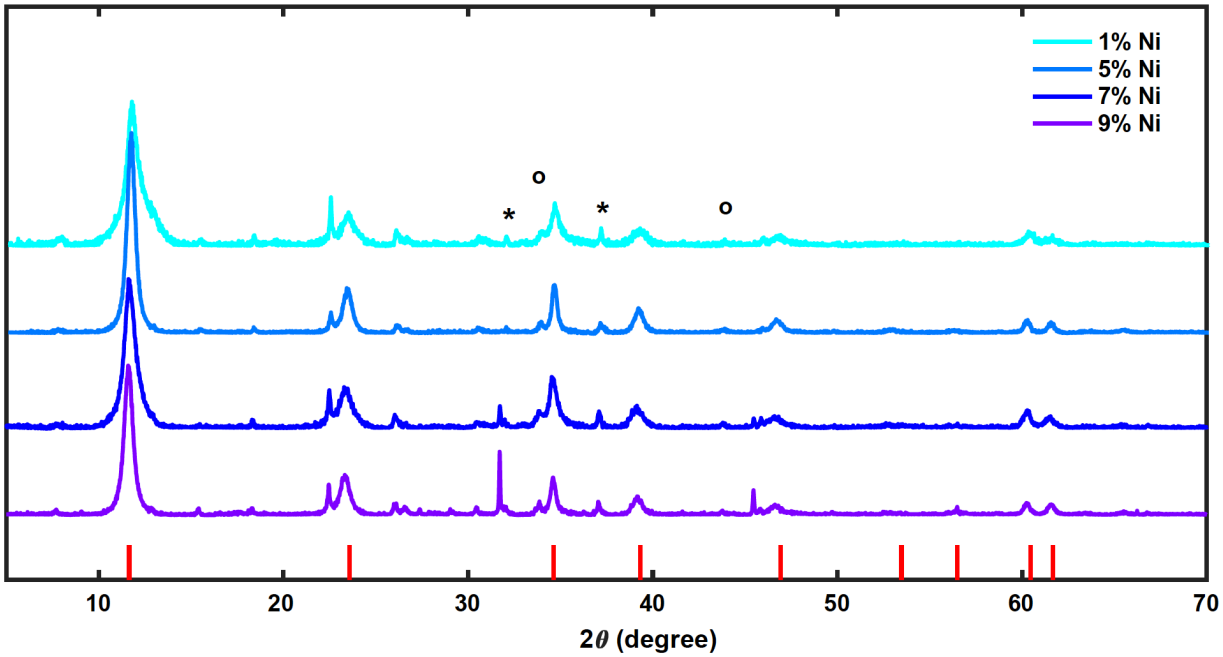

Figure S2. Powder XRD pattern of Ni-doped [ZnAl]-LDH with different concentrations of nickel. Black asterisks indicate peaks that corresponds to undoped [ZnAl]-LDH. Red lines: ZnAl layered double hydroxide (COD 9015034), *: ZnO (COD 2300113)

o: $Ni(OH)_2$ (COD 9012316)

III) ZFS determination by X-band CW EPR temperature dependence

Informed by the simulations, we can use the temperature dependence of the spectra to determine axial zero field splitting parameter (*D*). The positions of the major spectral features are due to transitions within the different Kramers doublets. The fractional populations of these Kramers doublets are determined by the Boltzmann distribution at any given temperature. By varying the temperature of the acquired spectra and monitoring the intensity of peaks that we have assigned to different Kramers doublets, we can extract the energy splitting between these doublets and thus determine *D*.[1,2]

In the hydrated and dehydrated 1%-[Fe:ZnAl]-LDH the peak at g_{eff} = 9 is assigned to the M_s=1/2 doublet and the peak at g_{eff} = 4.3 is assigned to the M_s=3/2 doublet of both B_H and B_D. In the dehydrated 1%-[Fe:ZnAl]-LDH the peak at g_{eff} = 6 is assigned to the M_s=1/2 doublet and the peak at g_{eff} = 2 is assigned to the M_s=3/2 doublet of species B_H and B_D. These peaks are not well resolved in the hydrated sample, which precludes the determination of *D* for hydrated species B by this technique. A plot of the logarithm of the relative intensities of the peaks (for the M_s=1/2 and M_s=3/2 doublets) *versus* the inverse of the temperature, the slope is equal to the energy splitting between these doublets (2*D*).

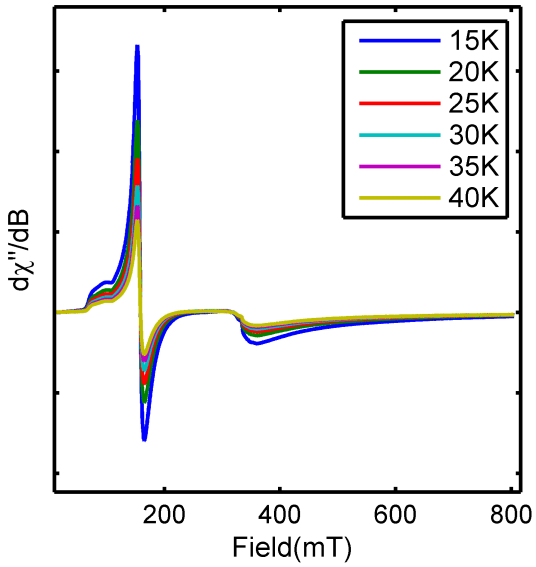

Figure S3. EPR spectra of dehydrated 1% [Fe:ZnAl]-LDH acquired at different temperatures. Spectra were acquired at 9.4 GHz and 502 μW power.

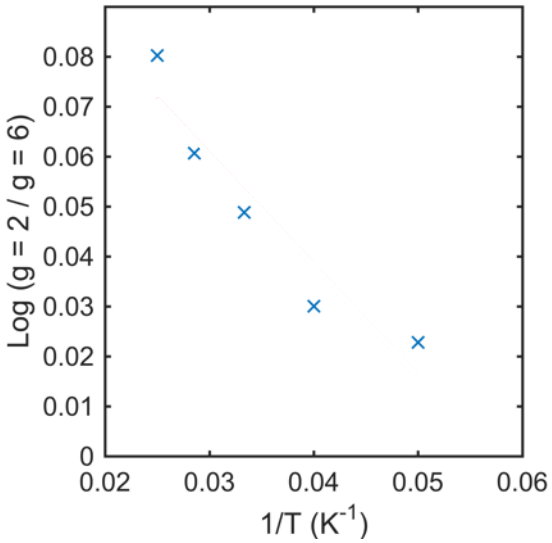

Figure S4. Plot of the logarithm of the ratio of peak intensities at 335 mT (*g* = 2) and 120 mT (*g* = 4.3) *versus* inverse temperature for dehydrated 1% [Fe:ZnAl]-LDH (blue). The negative slope infers that *D* is negative for species E_D.

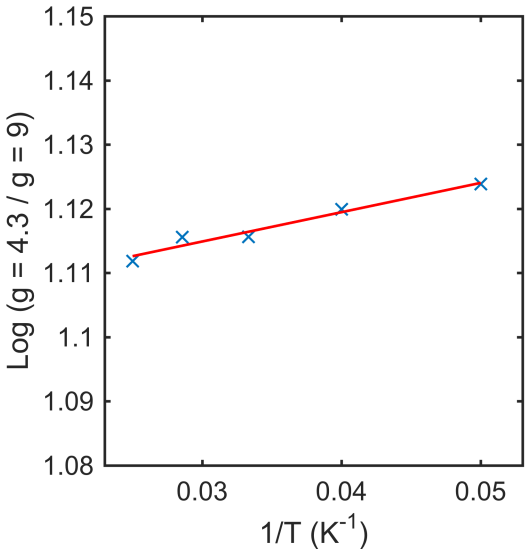

Figure S5. Plot of the logarithm of the ratio of peak intensities at 80 mT (*g* = 9) and 180 mT (*g* = 4.3) *versus* inverse temperature for dehydrated 1% [Fe:ZnAl]-LDH (blue) and a best-fit line (y=0.4569x + 1.1012 R^2 =0.96107) (red). The fit yields *D* = 0.20 cm^{-1} for species B_D.

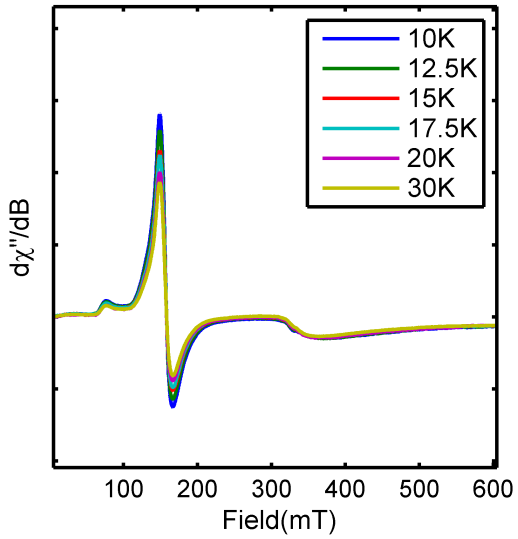

Figure S6. EPR spectra of hydrated 1% [Fe:ZnAl]-LDH acquired at different temperatures. Spectra acquired at 9.4 GHz and 502 μW power.

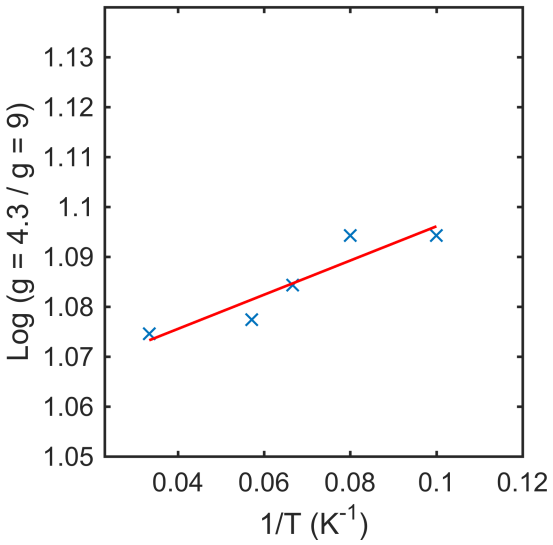

Figure S7. Plot of the logarithm of the ratio of peak intensities at 80 mT (*g* = 9) and 180 mT (*g* = 4.3) *versus* inverse temperature for hydrated 1% [Fe:ZnAl]-LDH (blue) and a best-fit line (y=0.3977x + 0.91387 R^2 =0.91387) (red). The fit yields *D* = 0.20 cm^{-1} for species B_H.

IV) Electrochemical characterization

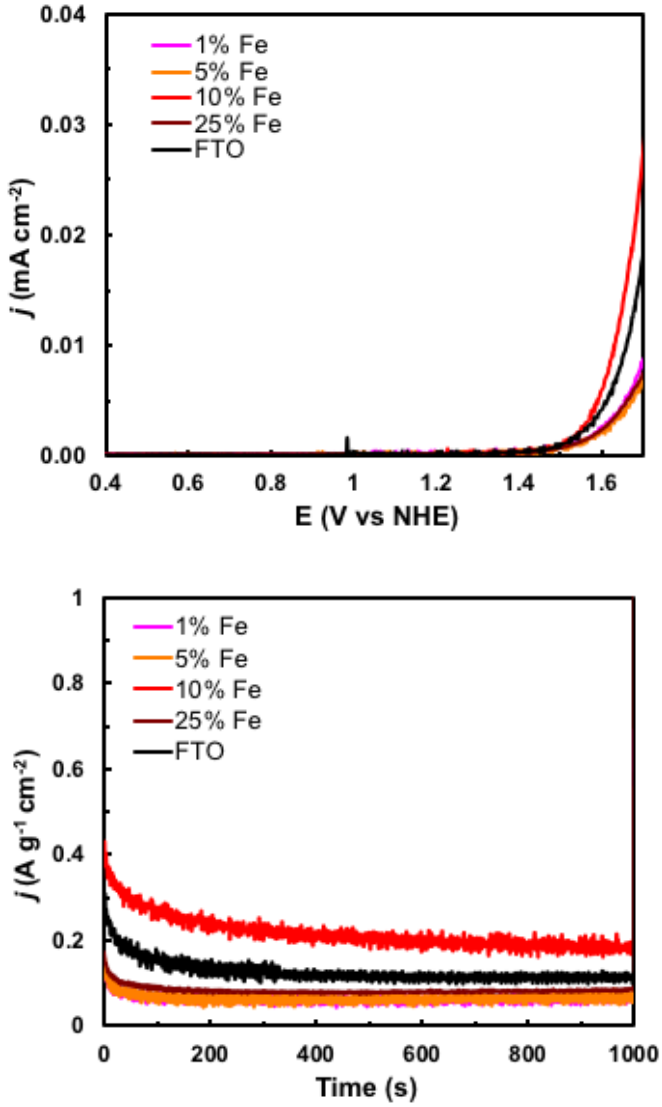

Figure S8. Top: Linear sweep voltammetry of [Fe:ZnAl]-LDH at varying Fe doping percentages. Scans began at the open circuit potential and swept anodically at a rate of 10 mV/s. Bottom: Chronoamperometry of [Fe:ZnAl]-LDH at varying Fe doping percentages. The working electrode was FTO-coated glass in 0.5 M potassium phosphate buffer at pH 7. Potential was held at 1.6 V vs NHE (η = 780 mV @ pH 7). Potentials were referenced to an Ag/AgCl (saturated KCl) electrode and converted to NHE.

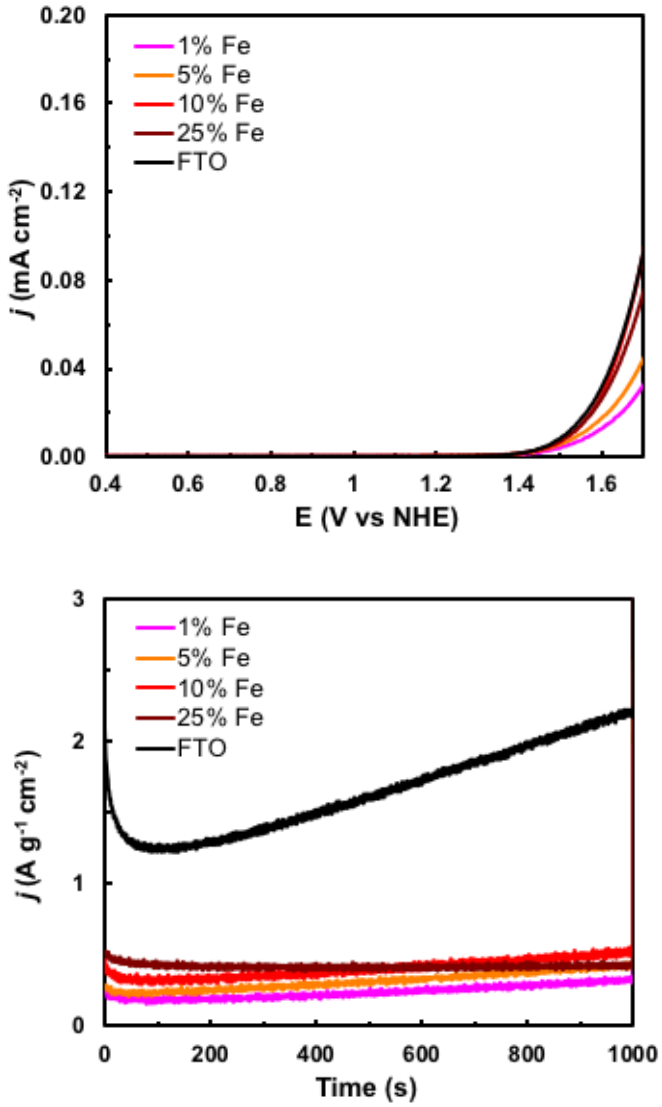

Figure S9. Top: Linear sweep voltammetry of [Fe:ZnAl]-LDH at varying Fe doping percentages. Scans began at the open circuit potential and swept anodically at a rate of 10 mV/s. Bottom: Chronoamperometry of [Fe:ZnAl]-LDH at varying Fe doping percentages. The working electrode was FTO-coated glass in 0.5 M potassium phosphate buffer at pH 9. Potential was held at 1.5 V vs NHE (η = 800 mV @ pH 9). Potentials were referenced to an Ag/AgCl (saturated KCl) electrode and converted to NHE.

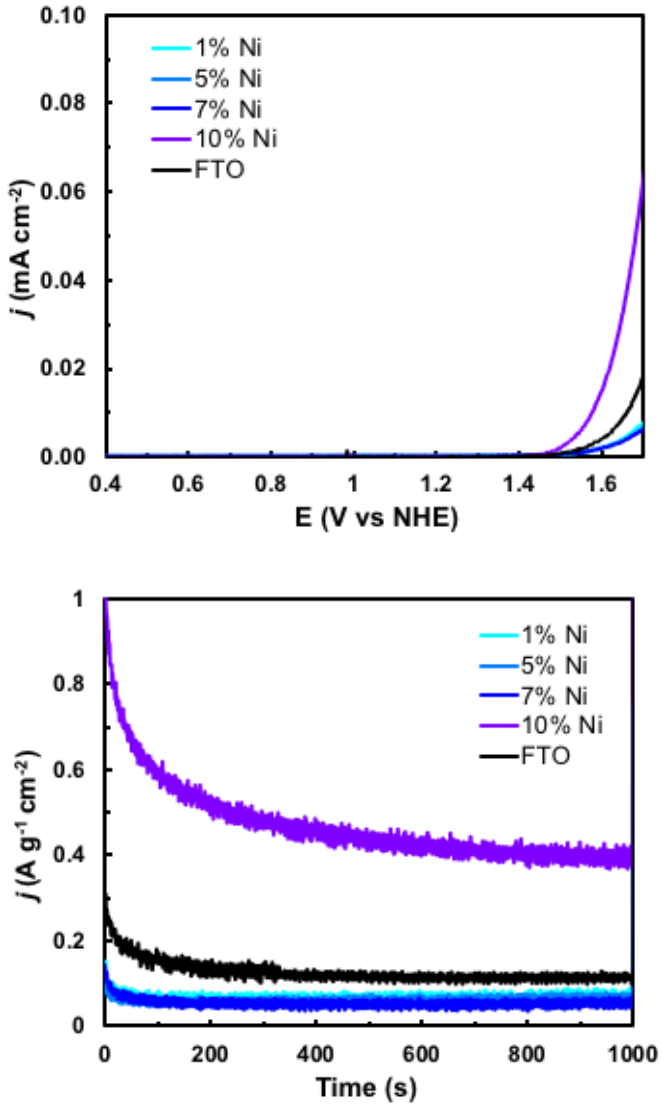

Figure S10. Top: Linear sweep voltammetry of [Ni:ZnAl]-LDH at varying Ni doping percentages. Scans began at the open circuit potential and swept anodically at a rate of 10 mV/s. Bottom: Chronoamperometry of [Ni:ZnAl]-LDH at varying Ni doping percentages. The working electrode was FTO-coated glass in 0.5 M potassium phosphate buffer at pH 7. Potential was held at 1.6 V vs NHE (η = 780 mV @ pH 7). Potentials were referenced to a Ag/AgCl (saturated KCl) electrode and converted to NHE.

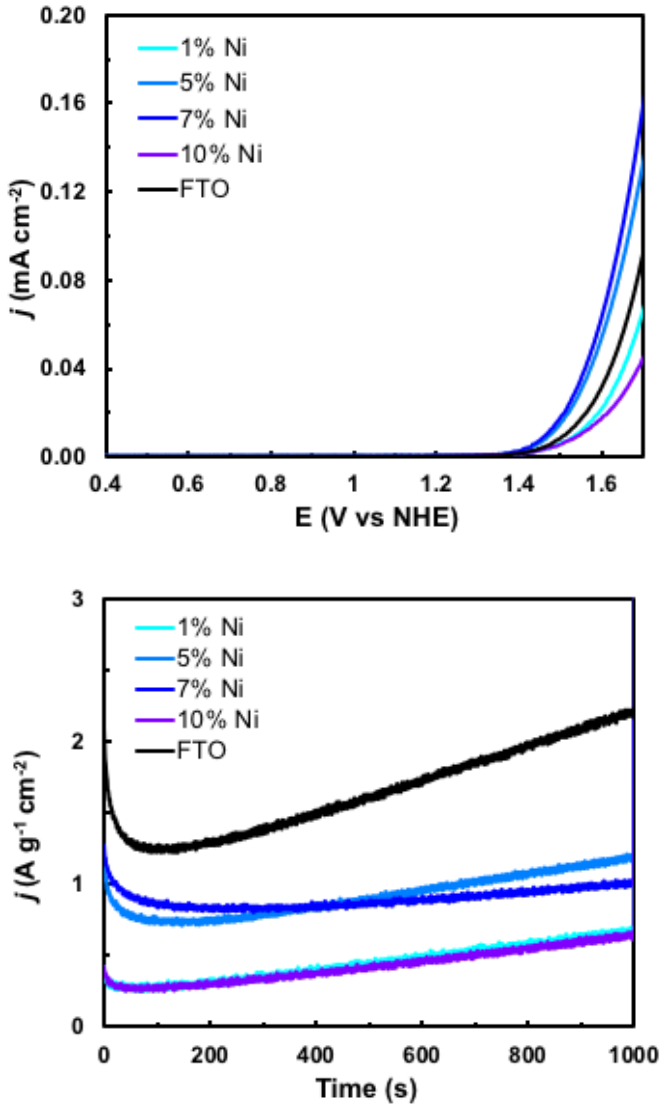

Figure S11. Top: Linear sweep voltammetry of [Ni:ZnAl]-LDH at varying Ni doping percentages. Scans began at the open circuit potential and swept anodically at a rate of 10 mV/s. Bottom: Chronoamperometry of [Ni:ZnAl]-LDH at varying Ni doping percentages. The working electrode was FTO-coated glass in 0.5 M potassium phosphate buffer at pH 9. Potential was held at 1.5 V vs NHE (η = 800 mV @ pH 9). Potentials were referenced to a Ag/AgCl (saturated KCl) electrode and converted to NHE.

V) References

(1) Blumberg, W. E.; Peisach, J. The Measurement of Zero Field Splitting and the Determination of Ligand Composition in Mononuclear Nonheme Iron Proteins. *Ann. N. Y. Acad. Sci.* **1973**, *222*, 539–560.

(2) Slappendel, S.; Veldink, G. A.; Vliegenthart, J. F. G.; Aasa, R.; Malmström, B. G. EPR Spectroscopy of Soybean Lipoxygenase-1 Determination of the Zero-Field Splitting Constants of High-Spin Fe(III) Signals from Temperature and Microwave Frequency Dependence. *Biochim. Biophys. Acta, Protein Struct.* **1980**, *624*, 30–39.